JCAMECH

Vol. 51, No. 1, June 2020, pp 122-128
DOI: 10.22059/jcamech.2020.300244.496

Investigation of instable fluid velocity in pipes with internal nanofluid flow based on Navier-Stokes equations

Mohammad Hosein Fakhar, Ahmad Fakhar, Hamidreza Tabatabaei and Hossein Nouri-Bidgoli*

Department of Mechanical Engineering, Kashan Branch, Islamic Azad University, Kashan, Iran

ARTICLE INFO

Article history:
Received: 1 April 2020
Accepted: 14 May 2020

Keywords:
Instable fluid velocity
Nanofluid
Pipe
Navier-Stokes
Hamilton's principle.

ABSTRACT

In this article, the instable fluid velocity in the pipes with internal nanofluid is studied. The fluid is mixed by SiO2, AL2O3, CuO and TiO2 nanoparticles in which the equivalent characteristic of nanofluid is calculated by rule of mixture. The force induced by the nanofluid is assumed in the radial direction and is obtained by Navier-Stokes equation considering viscosity of nanofluid. The displacements of the structure are described by first order shear deformation theory (FSDT). The final equations are calculated by Hamilton's principle. Differential quadrature method (DQM) is utilized for presenting the instable fluid velocity. The influences of length to radius ratio of pipe, volume fraction, diameter and type of nanoparticles are shown on the instable fluid velocity. The outcomes are compared with other published articles where shows good accuracy. Numerical results indicate that with enhancing the volume fraction of nanoparticles, the instable fluid velocity is increased. In addition, the instable fluid velocity of SiO2-water is higher than other types of nanoparticles assumed in this work.

1. Introduction

Instability is a destructive factor of the structures which can induce financial and psychological damages. One of the factors which create the instability is internal fluid flow in the pipelines. When the nanofluid velocity reaches to a special value, the structure will be instable which is very dangerous. However, investigation of instable fluid velocity in the pipes conveying fluid flow is very important for the optimum design of them. For this purpose, we focused on this subject in this article.

Most of the studies in the field of pipe conveying fluid are reviewed by Paidoussis [1] and Amabili [2]. Toorani and Lakis [3] studied the dynamic behaviour of cylindrical shells with internal fluid. A numerical solution was applied by Zhang et al. [4] for the dynamic response of ortho-cylindrical shells containing fluid flow utilizing Sanders' and classical theories. A new formulation was introduced by Jayaraj et al. [5] for the composite cylindrical shells with internal fluid. Zhang et al. [6] investigated vibration response of cylindrical shells with internal fluid. The interaction of fluid on the cylindrical shells with internal fluid flow was calculated by Kadoli and Ganesan [7] based on finite element method in order to buckling and vibration responses. Wang and Ni [8] investigated chaotic and stability analysis of standing pipe containing fluid utilizing numerical methods. The dynamic behaviour of fluid-conveying shells with simply supported boundary conditions was presented by Modarres-Sadeghi and Païdoussis [9]. Meng et al. [10] presented 3D nonlinear dynamics in fluid-conveying pipe utilizing numerical methods. The Differential Transformation Method (DTM) was utilized by Ni et al. [11] to investigate the vibration in the shells containing fluid with different boundary conditions. Vibration of 3D pipes containing fluid was formulated by Dai et al. [12] for calculating the structure frequency. A 3D exact solution was used by Gay-Balmaz and Putkaradze [13] for dynamics of tubes containing fluid. Nonlinear motion equations for fluid-conveying pipes were presented by Zhang et al. [14] assuming different boundary conditions. Dynamic analysis of a fluid-containing pipe was investigated by Gu et al. [15] utilizing Timoshenko theory of beam. The Galerkin method was studied by Li et al. [16] to dynamic analysis of pipe with internal fluid and under

* Corresponding author, Ph.D.,
E-mail: a.fakhar@iaukashan.ac.ir

moving load. Variable density fluid was simulated by Bai et al. [17] using novel mathematical model that satisfies the continuity of the fluid flow. Dynamic response of curved pipe with internal fluid and arbitrary un-deformed configuration was presented by Hu and Xhu [18].

In the field of mathematical modeling of structure, Daneshmehr et al. [19] used higher order theory for free vibration of functionally graded (FG) nanoplate. Zamani Nejad et al. [20-22] studied vibration and bending of FG nano-beams based on Euler-Bernoulli model. A review of FG thick cylindrical and conical shells was presented by Zamani Nejad et al. [23]. Hadi et al. [24, 25] and Zamani Nejad et al. [26] investigated vibration response of FG nanobeams utilizing different theories. Zarezadeh et al. [27] and Barati et al. [28] studied vibration of FG nano-rod and nanobeam subjected to magnetic field. Dehshahri et al. [29] investigated vibration response of FG nanoplate utilizing differential quadrature method. Static torsion analysis of FG microtube was presented by Barati et al. [30]. Noroozi et al. [31] studied torsional vibration analysis of bi-directional FG nano-cone.

In this paper, the instable fluid velocity in the pipes with internal fluid is presented for the first time. The nanofluid is mixed by SiO_2, AL_2O_3, CuO and TiO_2 nanoparticles in which the mixture rule is utilized for calculating the equivalent properties. Based on FSDT and Hamilton's principle, the final equations are obtained. DQM is used for solution for calculating the instable fluid velocity. The influences of length to radius ratio of pipe, volume fraction, diameter and type of nanoparticles are shown on the instable fluid velocity.

2. Mathematical modelling

Fig. 1 shows a pipe with radius R, length L and thickness h, which is conveying nanofluid. The pipe is located at both ends at supports. Our purpose in this work is mathematical modeling of structure and calculating the instable fluid velocity.

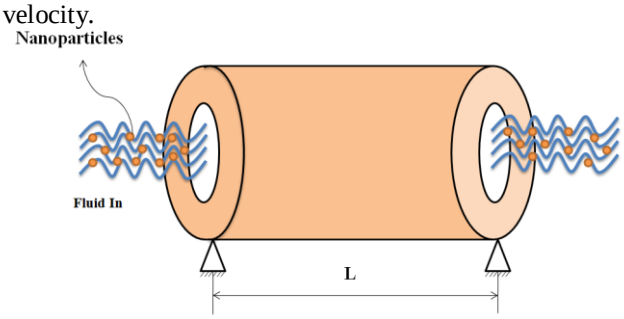

Figure 1. A pipe with internal nanofluid

Utilizing FSDT, the displacements of the pipe are [32]

$$u_x(x,\theta,z,t)=u\ (x,\theta,t)+z\psi_x(x,\theta,t), \tag{1}$$

$$u_\theta(x,\theta,z,t)=v(x,\theta,t)+z\psi_\theta(x,\theta,t), \tag{2}$$

$$w(x,\theta,z,t)=w(x,\theta,t), \tag{3}$$

where $(u(x,\theta,z,t),v(x,\theta,z,t),w(x,\theta,z,t))$ are the general displacements in (x,θ,z) directions, $(u(x,\theta,t),v(x,\theta,t),w(x,\theta,t))$ show the mid-plane displacements in (x,θ,z) directions, respectively; ψ_x and ψ_θ present the rotations about x- and θ- directions, respectively. The strain relations for the present system are

$$\varepsilon_{xx}=\frac{\partial u}{\partial x}+\frac{1}{2}\left(\frac{\partial w}{\partial x}\right)^2+z\frac{\partial \psi_x}{\partial x}, \tag{4}$$

$$\varepsilon_{\theta\theta}=\frac{\partial v}{R\partial\theta}+\frac{w}{R}+\frac{1}{2}\left(\frac{\partial w}{R\partial\theta}\right)^2+z\frac{\partial \psi_\theta}{R\partial\theta}, \tag{5}$$

$$\gamma_{x\theta}=\frac{\partial u}{R\partial\theta}+\frac{\partial v}{\partial x}+\frac{\partial w}{\partial x}\frac{\partial w}{R\partial\theta}+z\left(\frac{\partial \psi_x}{R\partial\theta}+\frac{\partial \psi_\theta}{\partial x}\right), \tag{6}$$

$$\gamma_{\theta z}=\frac{\partial w}{R\partial\theta}-\frac{v}{R}+\psi_\theta, \tag{7}$$

$$\gamma_{xz}=\frac{\partial w}{\partial x}+\psi_x. \tag{8}$$

Utilizing Hook's law, the stress relations are

$$\begin{Bmatrix}\sigma_{xx}\\ \sigma_{\theta\theta}\\ \sigma_{zz}\\ \sigma_{\theta z}\\ \sigma_{xz}\\ \sigma_{x\theta}\end{Bmatrix}=\begin{bmatrix}C_{11}&C_{12}&C_{13}&0&0&0\\ C_{12}&C_{22}&C_{23}&0&0&0\\ C_{13}&C_{12}&C_{33}&0&0&0\\ 0&0&0&C_{44}&0&0\\ 0&0&0&0&C_{55}&0\\ 0&0&0&0&0&C_{66}\end{bmatrix}\begin{Bmatrix}\varepsilon_{xx}\\ \varepsilon_{\theta\theta}\\ \varepsilon_{zz}\\ \gamma_{\theta z}\\ \gamma_{xz}\\ \gamma_{x\theta}\end{Bmatrix}, \tag{9}$$

where C_{ij} are elastic constants. The potential energy for the pipe conveying nanofluid is

$$U_P=\frac{1}{2}\int_0^{2\pi}\int_0^L\int_{-h/2}^{h/2}\begin{pmatrix}\sigma_{xx}\varepsilon_{xx}+\sigma_{\theta\theta}\varepsilon_{\theta\theta}+\sigma_{x\theta}\gamma_{x\theta}\\ +\sigma_{xz}\gamma_{xz}+\sigma_{\theta z}\gamma_{\theta z}\end{pmatrix}dzdxRd\theta. \tag{10}$$

Substituting Eqs. (4)-(8) into Eq. (10) yields

$$\begin{aligned}U=\frac{1}{2}\int_0^{2\pi}\int_0^L\Bigg\{&\left[N_{xx}\left(\frac{\partial u}{\partial x}+\frac{1}{2}\left(\frac{\partial w}{\partial x}\right)^2\right)+M_{xx}\frac{\partial \psi_x}{\partial x}\right]+\\ &\left[N_{\theta\theta}\left(\frac{\partial v}{R\partial\theta}+\frac{w}{R}+\frac{1}{2}\left(\frac{\partial w}{R\partial\theta}\right)^2\right)+M_{\theta\theta}\frac{\partial \psi_\theta}{R\partial\theta}\right]\\ &+Q_x\left(\psi_x+\frac{\partial w}{\partial x}\right)+N_{x\theta}\left[\frac{\partial u}{R\partial\theta}+\frac{\partial v}{\partial x}+\frac{\partial w}{\partial x}\frac{\partial w}{R\partial\theta}\right]\\ &+M_{x\theta}\left[\frac{\partial \psi_x}{R\partial\theta}+\frac{\partial \psi_\theta}{\partial x}\right]+Q_\theta\left[\frac{\partial w}{R\partial\theta}-\frac{v}{R}+\psi_\theta\right]\Bigg\}dA,\end{aligned} \tag{11}$$

where the stress resultant-displacement relations are

$$\begin{Bmatrix}N_{xx}\\ N_{\theta\theta}\\ N_{x\theta}\end{Bmatrix}=\int_{-\frac{h}{2}}^{\frac{h}{2}}\begin{Bmatrix}\sigma_{xx}\\ \sigma_{\theta\theta}\\ \tau_{x\theta}\end{Bmatrix}dz, \tag{12}$$

$$\begin{Bmatrix}Q_x\\ Q_\theta\end{Bmatrix}=k'\int_{-\frac{h}{2}}^{\frac{h}{2}}\begin{Bmatrix}\tau_{xz}\\ \tau_{y\theta}\end{Bmatrix}dz, \tag{13}$$

$$\begin{Bmatrix}M_{xx}\\ M_{\theta\theta}\\ M_{x\theta}\end{Bmatrix}=\int_{-\frac{h}{2}}^{\frac{h}{2}}\begin{Bmatrix}\sigma_{xx}\\ \sigma_{\theta\theta}\\ \tau_{x\theta}\end{Bmatrix}zdz \tag{14}$$

In which k' is shear correction factor. The kinetic energy of the structure is

$$\begin{aligned}K=\frac{1}{2}\int\Bigg(&I_0\left(\left(\frac{\partial u}{\partial t}\right)^2+\left(\frac{\partial v}{\partial t}\right)^2+\left(\frac{\partial w}{\partial t}\right)^2\right)\\ &+I_1\left(2\frac{\partial u}{\partial t}\frac{\partial \psi_x}{\partial t}+2\frac{\partial v}{\partial t}\frac{\partial \psi_\theta}{\partial t}\right)\\ &+I_2\left(\left(\frac{\partial \phi_x}{\partial t}\right)^2+\left(\frac{\partial \phi_y}{\partial t}\right)^2\right)\Bigg)dA.\end{aligned} \tag{15}$$

here the moments of inertias are

$$\begin{Bmatrix} I_0 \\ I_1 \\ I_2 \end{Bmatrix} = \int_{-h/2}^{h/2} \begin{bmatrix} \rho \\ \rho z \\ \rho z^2 \end{bmatrix} dz, \tag{16}$$

The governing equation of the fluid can be presented by the well-known Navier-Stokes equation as follows [33]

$$\rho_e \frac{d\mathrm{V}}{dt} = -\nabla \mathrm{P} + \mu_e \nabla^2 \mathrm{V} + \mathrm{F}_{body}, \tag{17}$$

where $V \equiv (v_z, v_\theta, v_x)$ is the flow velocity vector; P, μ_e and ρ_e are respectively the pressure, nanofluid influenceive viscosity and nanofluid influenceive density; F_{body} denotes the body forces. In addition, the total derivative operator with respect to *t* can be given as

$$\frac{d}{dt} = \frac{\partial}{\partial t} + v_x \frac{\partial}{\partial x} + v_\theta \frac{\partial}{R\partial \theta} + v_z \frac{\partial}{\partial z}. \tag{18}$$

At the contact between the fluid and the pipe, we have the following boundary condition

$$v_z = \frac{dw}{dt}. \tag{19}$$

Combining Eqs. (17)-(19), the radial force induced by the nanofluid flow can be obtained as

$$\begin{aligned} F_{fluid} = A\frac{\partial p_z}{\partial z} = -\rho_e \left(\frac{\partial^2 w}{\partial t^2} + 2v_x \frac{\partial^2 w}{\partial x \partial t} + {v_x}^2 \frac{\partial^2 w}{\partial x^2} \right) \\ + \mu_e \left(\frac{\partial^3 w}{\partial x^2 \partial t} + \frac{\partial^3 w}{R^2 \partial \theta^2 \partial t} + v_x \left(\frac{\partial^3 w}{\partial x^3} + \frac{\partial^3 w}{R^2 \partial \theta^2 \partial x} \right) \right). \end{aligned} \tag{20}$$

However, the external work of the nanofluid flow can be written as

$$\begin{aligned} W = \int (F_{fluid}) w dA = \int \left(-\rho_e \left(\frac{\partial^2 w}{\partial t^2} + 2v_x \frac{\partial^2 w}{\partial x \partial t} + {v_x}^2 \frac{\partial^2 w}{\partial x^2} \right) \right. \\ \left. + \mu_e \left(\frac{\partial^3 w}{\partial x^2 \partial t} + \frac{\partial^3 w}{R^2 \partial \theta^2 \partial t} + v_x \left(\frac{\partial^3 w}{\partial x^3} + \frac{\partial^3 w}{R^2 \partial \theta^2 \partial x} \right) \right) \right) w dA. \end{aligned} \tag{21}$$

The influenceive density and viscosity of the nanofluid based on mixture rule are [34]

$$\rho_e = (1-\phi)\rho_f + \phi \rho_p, \tag{22}$$

$$\mu_e = \left(1 + 39.11\phi + 533.9\phi^2\right)\mu_f, \tag{23}$$

where ϕ is the nanoparticles volume fraction; ρ_p is the density of nanoparticles; μ_f is the viscosity of water which can be given as

$$\mu_f = 2.414 \times 10^{-5} \times 10^{\frac{247.8}{T-140}} \tag{24}$$

where *T* is in Kelvin and is room temperature.

Applying Hamilton's principal we have

$$\int_0^t (\delta U - \delta K - \delta W) dt = 0, \tag{25}$$

the motion equations can be derived as

$$\delta u: \quad \frac{\partial N_{xx}}{\partial x} + \frac{\partial N_{x\theta}}{R\partial \theta} + R_x^m = I_0 \frac{\partial^2 u}{\partial t^2} + I_1 \frac{\partial^2 \psi_x}{\partial t^2}, \tag{26}$$

$$\delta v: \quad \frac{\partial N_{x\theta}}{\partial x} + \frac{\partial N_{\theta\theta}}{R\partial \theta} + \frac{Q_\theta}{R} + R_\theta^m = I_0 \frac{\partial^2 v}{\partial t^2} + I_1 \frac{\partial^2 \psi_\theta}{\partial t^2}, \tag{27}$$

$$\begin{aligned} \delta w: \quad & \frac{\partial Q_x}{\partial x} + \frac{\partial Q_\theta}{R\partial \theta} - \rho_e \left(\frac{\partial^2 w}{\partial t^2} + 2v_x \frac{\partial^2 w}{\partial x \partial t} + {v_x}^2 \frac{\partial^2 w}{\partial x^2} \right) \\ & + \mu_e \left(\frac{\partial^3 w}{\partial x^2 \partial t} + \frac{\partial^3 w}{R^2 \partial \theta^2 \partial t} + v_x \left(\frac{\partial^3 w}{\partial x^3} + \frac{\partial^3 w}{R^2 \partial \theta^2 \partial x} \right) \right) = I_0 \frac{\partial^2 w}{\partial t^2}, \end{aligned} \tag{28}$$

$$\delta \psi_x: \quad \frac{\partial M_{xx}}{\partial x} + \frac{\partial M_{x\theta}}{R\partial \theta} - Q_x + M_x^m = I_1 \frac{\partial^2 u}{\partial t^2} + I_2 \frac{\partial^2 \psi_x}{\partial t^2}, \tag{29}$$

$$\delta \psi_\theta: \quad \frac{\partial M_{x\theta}}{\partial x} + \frac{\partial M_{\theta\theta}}{R\partial \theta} - Q_\theta + M_\theta^m = I_1 \frac{\partial^2 v}{\partial t^2} + I_2 \frac{\partial^2 \psi_\theta}{\partial t^2}, \tag{30}$$

3. Solution method

Utilizing DQM, the differential motion equations can be transformed into algebraic ones by the below relations [35]

$$\frac{d^n F(x_i, \theta_j)}{dx^n} = \sum_{k=1}^{N_x} A_{ik}^{(n)} F(x_k, \theta_j) \qquad n = 1, ..., N_x - 1, \tag{31}$$

$$\frac{d^m F(x_i, \theta_j)}{d\theta^m} = \sum_{l=1}^{N_\theta} B_{jl}^{(m)} F(x_i, \theta_l) \qquad m = 1, ..., N_\theta - 1, \tag{32}$$

$$\frac{d^{n+m} F(x_i, \theta_j)}{dx^n d\theta^m} = \sum_{k=1}^{N_x} \sum_{l=1}^{N_\theta} A_{ik}^{(n)} B_{jl}^{(m)} F(x_k, \theta_l), \tag{33}$$

where $A_{ik}^{(n)}$ and $B_{jl}^{(m)}$ are the weighting coefficients which are

$$A_{ij}^{(1)} = \begin{cases} \dfrac{M(x_i)}{(x_i - x_j) M(x_j)}, & for \quad i \neq j, \quad i, j = 1, 2, ..., N_x \\ -\sum\limits_{\substack{j=1 \\ i \neq j}}^{N_x} A_{ij}^{(1)}, & for \quad i = j, \quad i, j = 1, 2, ..., N_x \end{cases} \tag{34}$$

$$B_{ij}^{(1)} = \begin{cases} \dfrac{P(\theta_i)}{(\theta_i - \theta_j) P(\theta_j)}, & for \quad i \neq j, \quad i, j = 1, 2, ..., N_\theta, \\ -\sum\limits_{\substack{j=1 \\ i \neq j}}^{N_\theta} B_{ij}^{(1)}, & for \quad i = j, \quad i, j = 1, 2, ..., N_\theta \end{cases} \tag{35}$$

where

$$M(x_i) = \prod_{\substack{j=1 \\ j \neq i}}^{N_x} (x_i - x_j), \tag{36}$$

$$P(\theta_i) = \prod_{\substack{j=1 \\ j \neq i}}^{N_\theta} (\theta_i - \theta_j). \tag{37}$$

In addition, N_θ and N_θ are the grid points number in x and θ directions respectively, which can be defined by Chebyshev polynomials as

$$x_i = \frac{L}{2}\left[1 - \cos\left(\frac{i-1}{N_x - 1}\right)\pi\right], \quad i = 1, ..., N_x \tag{38}$$

$$\theta_i = \frac{2\pi}{2}\left[1 - \cos\left(\frac{i-1}{N_\theta - 1}\right)\pi\right]. \quad i = 1, ..., N_\theta \tag{39}$$

However, applying DQM, we have the following coupled motion equations

$$[M]\begin{bmatrix} \ddot{Y}_b \\ \ddot{Y}_d \end{bmatrix} + [C]\begin{bmatrix} \dot{Y}_b \\ \dot{Y}_d \end{bmatrix} + [K_L + K_{NL}]\begin{bmatrix} Y_b \\ Y_d \end{bmatrix} = \begin{bmatrix} 0 \\ 0 \end{bmatrix}, \tag{40}$$

where $[K]$ and $[K_{NL}]$ are the linear and nonlinear stiffness matrixes, respectively; $[C]$ is the damp matrix; $[M]$ is the mass matrix; $\{Y\}$ is the displacement vector subscript b and d represent boundary and domain points. Finally, using eigenvalue problem, the frequency and instable fluid velocity of the structure can be derived.

4. Numerical result and dissection

A pipe with thickness to radius ratio and length to radius ratio of the pipe are *h/R=0.02* and *L/R=4*, respectively is

assumed made from Poly methyl methacrylate (PMMA) with Poisson's ratios and Young moduli of $\nu = 0.34$ and $E = 2.5GPa$, respectively. The inside fluid is water mixed by SiO_2, AL_2O_3, CuO and TiO_2 nanoparticles with the thermo-physical properties listed in Table 1 [36-40].

Table 1: Thermo-physical properties of water and nanoparticles [36-40]

	k(W/ mK)	$c_p(J/kg\,\mathrm{K})$	$\rho(kg/m^3)$
Water	0.61	4179	997.1
AL_2O_3	25	765	3970
CuO	69	535.6	6350
SiO_2	36	765	3970
TiO_2	13.7	683	4170

For validation of our results, the nanofluid is neglected and frequency of classical cylindrical shells is obtained based on DQM. The pipe parameters of the classical theory assumed as $h/R = 0.01$, $L/R = 20$, $E = 210GPa$, $\nu = 0.3$, $\rho = 7850\ Kg/m^3$. A shown in Table 2, the obtained outcomes are in a good agreement to those expressed in Qu et al. [40] and Zeinali Heris et al. [40], showing validation of this article.

Table 2: Validation of present work

n	Qu et al. [40]	Zeinali Heris et al. [40]	Present
1	0.016103	0.016101	0.016234
2	0.009382	0.011225	0.011714
3	0.022105	0.022310	0.024903
4	0.042095	0.042139	0.044935
5	0.068008	0.068024	0.070857
6	0.099730	0.099738	0.102591
7	0.137239	0.137240	0.140108
8	0.180528	0.180530	0.183402
9	0.229594	0.229596	0.232472
10	0.284436	0.284439	0.287318

Figs. 2 and 3 show the volume fraction of nanoparticles in fluid on the frequency ($\mathrm{Im}(\Omega)$) and damping ($\mathrm{Re}(\Omega)$) of structure ($\Omega = \sqrt{C_{11}/\rho_f}\,\omega$) versus fluid velocity, respectively. It can be found that the frequency reduces with enhancing fluid velocity, while the damping is zero. These show that the structure is stable. When the frequency reaches to zero, instable fluid velocity has append . In this state, the damping has two answers of positive and negative which makes the structure unstable. Furthermore, enhancing nanoparticles volume fraction leads to increase in the instable fluid velocity.

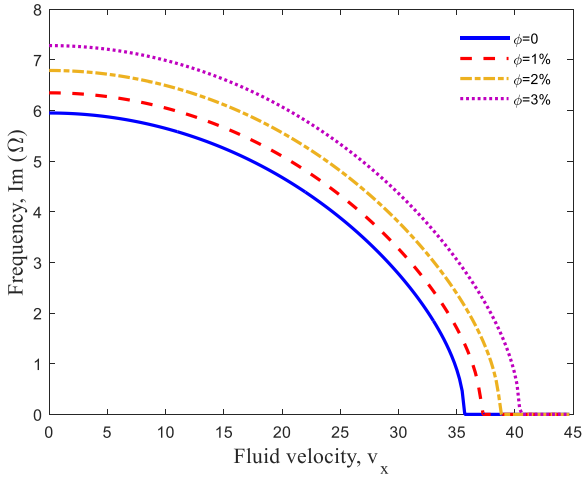

Figure 2. The influence of volume fraction of nanoparticles on the structure frequency

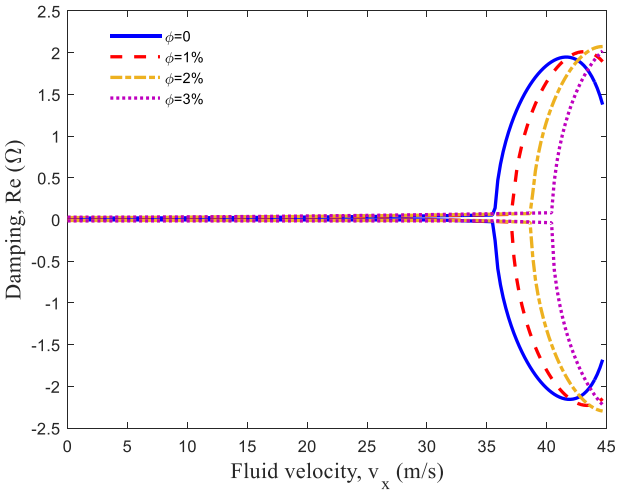

Figure 3. The influence of volume fraction of nanoparticles on the structure damping

The influence of diameter of nanoparticles is indicated in Fig. 4 and 5 on the non-dimensional frequency and damping of the pipe. It is found that with enhancing the diameter of nanoparticles, the frequency and instable fluid velocity are decreased. It is because with enhancing the diameter of nanoparticles, the thermo-physical properties of nanoparticles decrease.

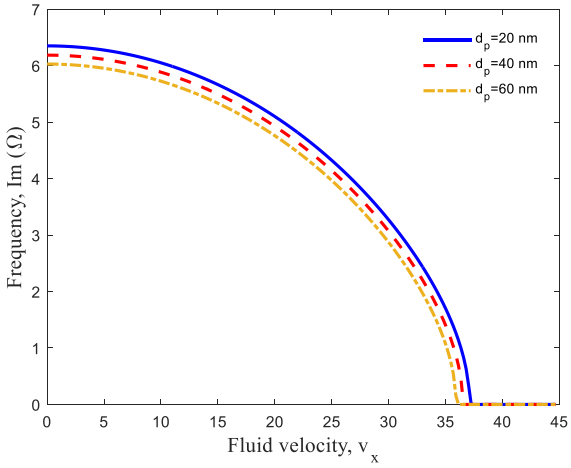

Figure 4. The influence of diameter of nanoparticles on the structure frequency

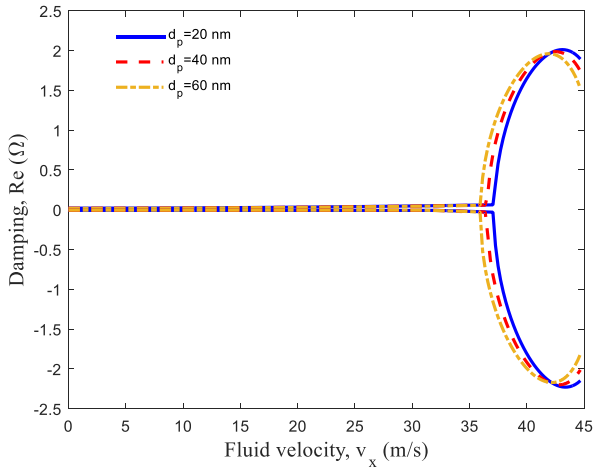

Figure 5. The influence of diameter of nanoparticles on the structure damping

In realizing the influence of nanoparticles type, Figs. 6 and 7 show how non-dimensional frequency and damping of the pipe changes versus the fluid velocity. It is found that from Fig. 4, the frequency and instable fluid velocity for the SiO_2 nanoparticles are maximum in comparison with other types of nanoparticles. It is due to good thermo-physical properties of SiO_2 nanoparticles with respect to AL_2O_3, CuO and TiO_2 nanoparticles.

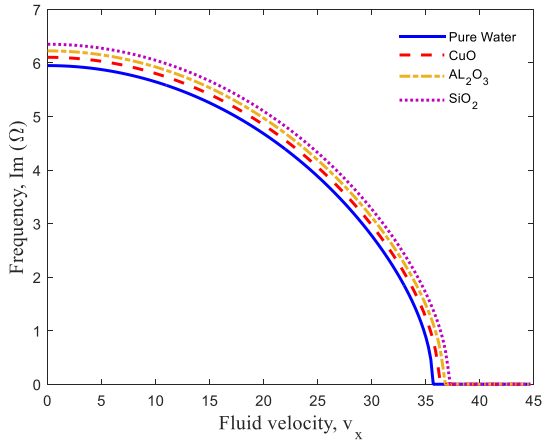

Figure 6. The influence of nanoparticles type on the structure frequency

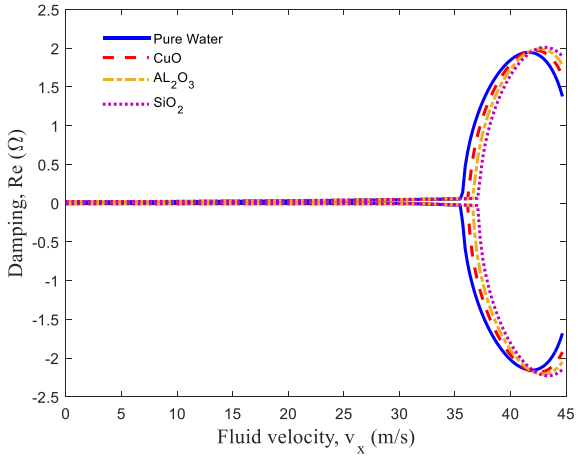

Fig. 7 The influence of nanoparticles type on the structure damping

Figs. 8 and 9 illustrate the influence of length to radius ratio on the Im(Ω) and Re(Ω) versus fluid velocity, respectively. The results indicate that with enhancing length to radius ratio, the frequency and instable fluid velocity are decreased. It is since with enhancing length to radius ratio, the stiffness of structure is reduced.

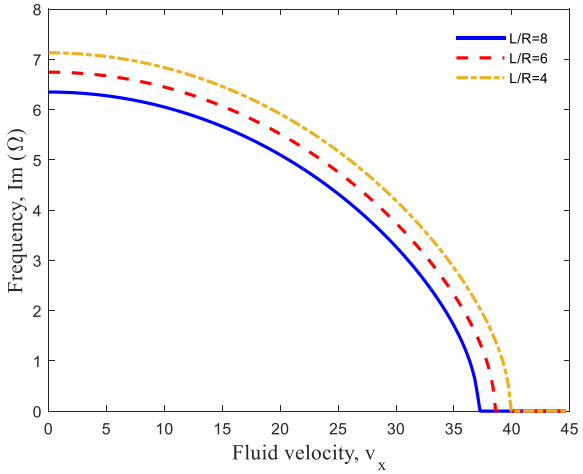

Figure 8. The influence of length to radius ratio on the structure frequency

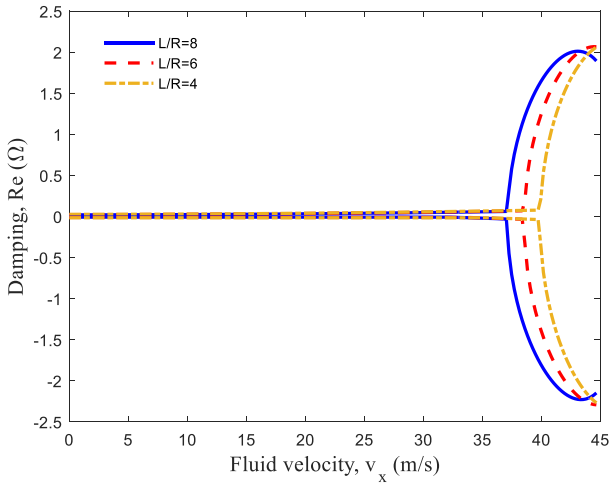

Figure 9. The influence of length to radius ratio on the structure damping

5. Conclusion

Instable fluid velocity in pipe conveying nanofluid was investigated in this study based on mathematical model. The nanofluid was mixed by SiO_2, AL_2O_3, CuO and TiO_2 nanoparticles based on mixture rule. The pipe was modelled by FSDT and the final equations were derived by Hamilton's principle. DQM was applied for calculating the instable fluid velocity. The effects of length to radius ratio of pipe, volume fraction, diameter and type of nanoparticles were shown on the instable fluid velocity. Results show that enhancing volume fraction of nanoparticles in fluid leads to increase in the instable fluid velocity. It can be seen that with enhancing the diameter of nanoparticles, the frequency and instable fluid velocity were decreased. In addition, the frequency and instable fluid velocity for the SiO_2 nanoparticles were maximum with respect to other type of nanoparticles. Furthermore, with enhancing length to radius ratio, the frequency and instable fluid velocity were decreased.

Reference

[1] Paidoussis M.P., Li G.X., 1993, Pipes conveying fluid: a model dynamical problem, *Journal of Fluids and Structures*, **7**: 137–204.

[2] Amabili M., 2008, Nonlinear Vibrations and Stability of Shells and Plates, Cambridge University Press, New York.

[3] Toorani M.H., Lakis A.A., 2001, Dynamic analysis of anisotropic cylindrical shells containing flowing fluid, *Journal of Pressure Vessels and Technology Transection ASME*, **123**: 454–60.

[4] Zhang X.M., Liu G.R., Lam K.Y., 2001, Frequency analysis of cylindrical panels using a wave propagation approach, *Applied Acoustics*, **62**: 527–543.

[5] Jayaraj K., Ganesan N., Chandramouli P., 2002, A semi-analytical coupled finite element formulation for composite shells conveying fluids, *Journal of Sound and Vibration*, **258**: 287–307.

[6] Zhang Y.L., Reese J.M., Gorman D.G., 2002, Initially tensioned orthotropic cylindrical shells conveying fluid: A vibration analysis, *Journal of Fluids and Structures*, **16**1: 53–70,.

[7] Kadoli R., Ganesan N., 2003 وFree vibration and buckling analysis of composite cylindrical shells conveying hot fluid, *Composite Structures*, **60**: 19–32.

[8] Wang L., Ni Q., 2006, A note on the stability and chaotic motions of a restrained pipe conveying fluid, *Journal of Sound and Vibration*, **296**: 1079–1083.

[9] Modarres-Sadeghi Y., Païdoussis M.P., 2009, Nonlinear dynamics of extensible fluid-conveying pipes, supported at both ends, *Journal of Fluids and Structures*, **25**: 535-543.

[10] Meng D., Guo H., Xu S., 2011, Non-linear dynamic model of a fluid-conveying pipe undergoing overall motions, *Applied Mathematical Modelling*, **35:**, pp. 781-796.

[11] Ni Q., Zhang Z.L., Wang L., 2011 وApplication of the differential transformation method to vibration analysis of pipes conveying fluid, *Applied Mathematical and Computation*, **217**: 7028-7038.

[12] Dai H.L., Wang L., Qian Q., Gan J., 2012, Vibration analysis of three-dimensional pipes conveying fluid with consideration of steady combined force by transfer matrix method, *Applied Mathematical and Computation* **219**: 2453-2464.

[13] Gay-Balmaz F., Putkaradze V., 2015, On flexible tubes conveying fluid: geometric nonlinear theory, stability and dynamics, *Journal of Nonlinear Science*, **25**: 889-936.

[14] Zhang T., Ouyang H., Zhang Y.O., Lv B.L., 2016, Nonlinear dynamics of straight fluid-conveying pipes with general boundary conditions and additional springs and masses, *Applied Mathematical Modelling*, 40: 7880-7900.

[15] Gu J., Tianqi M., Menglan, D., 2016, Influence of aspect ratio on the dynamic response of a fluid-conveying pipe using the Timoshenko beam model, *Ocean Engineering*, **114**: 185–191.

[16] Li B., Wang Zh., Jing L., 2018, Dynamic Response of Pipe Conveying Fluid with Lateral Moving Supports, *Shock and Vibration*, **24**: ID 3295787.

[17] Bai Y., Xie W., Gao W., Xu W., 2018, Dynamic analysis of a cantilevered pipe conveying fluid with density variation, *Journal of Fluids and Structures*, **81**: 638-655.

[18] Hu Y.J., Zhu W., 2018, Vibration analysis of a fluid-conveying curved pipe with an arbitrary undeformed configuration, *Applied Mathematical Modelling*, **64**: 624-642.

[19] Daneshmehr, A., Rajabpoor, A., Hadi, A., 2015, Size dependent free vibration analysis of nanoplates made of functionally graded materials based on nonlocal elasticity theory with high order theories, *International Journal of Engineering Science*, **95**: 23-35.

[20] Zamani Nejad, M., Hadi, A., 2016, Non-local analysis of free vibration of bi-directional functionally graded Euler-Bernoulli nano-beams, *International Journal of Engineering Science*, **105**: 1-11.

[21] Zamani Nejad, M., Hadi, A., 2016, Eringen's non-local elasticity theory for bending analysis of bi-directional functionally graded Euler-Bernoulli nano-beams, *International Journal of Engineering Science*, **106**: 1-9.

[22] Zamani Nejad و M., Hadi A., Farajpour A., 2017, Consistent couple-stress theory for free vibration analysis of Euler-Bernoulli nano-beams made of arbitrary bi-directional functionally graded materials, *Structural Engineering and Mechanics* **63(**2): 161-169.

[23] Zamani Nejad M., Jabbari M., Hadi A., 2017, A review of functionally graded thick cylindrical and conical shells, *Journal of Computational Applied Mechanics* و**48**(2): 357-370.

[24] Hadi A., Zamani Nejad M., Hosseini M., 2018, Vibrations of three-dimensionally graded nanobeams, *International Journal of Engineering Science*, **128**: 12-23.

[25] Hadi A., Zamani Nejad M., Rastgoo A., Hosseini M., 2018, Buckling analysis of FGM Euler-Bernoulli nano-beams with 3D-varying properties based on consistent couple-stress theory, *Steel and Composite Structures*, **26**(6): 663-672.

[26] Zamani Nejad M., Hadi A., Omidvari A., Rastgoo A., 2018, Bending analysis of bi-directional functionally graded Euler-Bernoulli nano-beams using integral form of Eringen's non-local elasticity theory, *Structural Engineering and Mechanics*, **67**(4): 417-425.

[27] Zarezadeh E., Hosseini V., Hadi A., 2019, Torsional vibration of functionally graded nano-rod under magnetic field supported by a generalized torsional foundation based on nonlocal elasticity theory, *Mechanics Based Design of Structures and Machines*, **25**: 1-16.

[28] Barati A., Hadi A., Zamani Nejad M., Noroozi R., 2020, On vibration of bi-directional functionally graded nanobeams under magnetic field, *Mechanics Based Design of Structures and Machines*, **23**: 1-18.

[29] Dehshahri K., Zamani Nejad M., Ziaee S., Niknejad A., Hadi A., 2020, Free vibrations analysis of arbitrary three-dimensionally FGM nanoplates, *Advances in nano research*, **8**(2): 115-134.

[30] Barati A., Adeli M.M., Hadi A., 2020, Static torsion of bi-directional functionally graded microtube based on the couple stress theory under magnetic field, *International Journal of Applied Mechanics*, **12**(02): 2050021.

[31] Noroozi R., Barati A., Kazemi A., Norouzi S., Hadi A., 2020, Torsional vibration analysis of bi-directional FG nano-cone with arbitrary cross-section based on nonlocal strain gradient elasticity, *Advances in nano research*, **8**(1): 13-24.

[32] Brush, D.O., Almroth, B.O. 1975, Buckling of bars, plates and shells, McGraw-Hill, New York.

[33] Baohui, L., Hangshan, G., Yongshou, L., Zhufeng, Y., 2012, Free vibration analysis of micropipe conveying fluid by wave method, *Results in Physics*, **2**: 104–109.

[34] Sheikhzadeh G.A., Teimouri H., Mahmoodi M., 2013, Numerical study of mixed convection of nanofluid in a

concentric annulus with rotating inner cylinder, *Trans. Phenomen. Nano Micro Scales* **1**: 26-36.

[35] Bellman R., Casti J., 1971, Differential quadrature and long-term integration, *Journal of Mathematical Analysis and Applications*, **34**: 235–238.

[36] Eiamsa-ard S., Kiatkittipong K., Jedsadaratanachai W., 2015, Heat transfer enhancement of TiO2/water nanofluid in a heat exchanger tube equipped with overlapped dual twisted-tapes, *Engineering Science and Technology, an International Journal* **18**: 336-350.

[37] Kefayati G.R., Hosseinizadeh S.F., Gorji M., Sajjadi H., 2011, Lattice Boltzmann simulation of natural convection in tall enclosures using water/SiO2 nanofluid, *International Communications in Heat and Mass Transfer*, **38**: 798–805.

[38] Abu-Nada E., 2009, Influences of variable viscosity and thermal conductivity of Al2O3-water nanofluid on heat transfer enhancement in natural convection, *International Journal of Heat and Fluid Flow*, **30**: 679-690.

[39] Zeinali Heris S., Talaii E., Noie S.H., 2012, CuO/ Water Nanofluid Heat Transfer Through Triangular Ducts, *Iranian Journal of Chemical Engineering*, **9**, 23-33.

[40] Qu, Y., Chen, Y., Long, X., Hua, H., Meng, G. 2013, Free and forced vibration analysis of uniform and stepped circular cylindrical shells using a domain decomposition method, *Applied Acoustics*, **74**: 425–439.